

## Preparation, structure and catalytic properties of copper-zinc ferrites

K. V. Koleva<sup>1</sup>, N. I. Velinov<sup>1\*</sup>, T. S. Tsoncheva<sup>2</sup>, I. G. Mitov<sup>1</sup>

<sup>1</sup> Institute of Catalysis, BAS, Sofia, 1113, Bulgaria

<sup>2</sup> Institute of Organic Chemistry with Centre of Phytochemistry, BAS, Sofia, 1113, Bulgaria

Received December, 2014; Revised January, 2015

Well crystallized  $\text{Cu}_{1-x}\text{Zn}_x\text{Fe}_2\text{O}_4$  ferrites with different composition were prepared and tested as catalysts in methanol decomposition to CO and hydrogen. The influence of cation distribution in ferrites on their catalytic behaviour and phase transitions under the reaction medium was in the focus of the study. It was established that  $\text{Cu}_{0.8}\text{Zn}_{0.2}\text{Fe}_2\text{O}_4$  ferrite exhibits the highest catalytic activity and good selectivity in methanol decomposition to  $\text{H}_2$  and CO. Mössbauer study of samples after the catalytic test reveals transformation of the initial ferrite phase with the formation of Zn-substituted magnetite, iron carbide, wuestite and  $\alpha$ -Fe in different ratio.

**Key words:** copper-zinc ferrite, Mössbauer spectroscopy, methanol decomposition.

### INTRODUCTION

Ferrite materials are object of many scientific investigations because of their potential application in biology [1], electronics [2–4] and catalysis [5–13]. The spinel ferrites are usually denoted with general formula  $\text{AB}_2\text{O}_4$ . The distribution of metal ions in the spinel crystal lattice determines ferrite structure as normal, inverse and partial inverse spinel type. In the  $\text{ZnFe}_2\text{O}_4$  ferrite the tetrahedral (A)-sites are occupied by only one type of cations. This is because of the preferences of  $\text{Zn}^{2+}$  to occupy the tetrahedral spinel sites forming normal spinel, while  $\text{Cu}^{2+}$  occupies mainly the octahedral [B]-sites, and thus, the tetrahedral sites are occupied by half of  $\text{Fe}^{3+}$  and  $\text{CuFe}_2\text{O}_4$  describes as inverse spinel. In the case of  $\text{Cu}_{1-x}\text{Zn}_x\text{Fe}_2\text{O}_4$ , where  $0 < x < 1$ , the tetrahedral sites are occupied both by  $\text{Zn}^{2+}$  and  $\text{Fe}^{3+}$  cations and its spinel structure are denoted as partially inverse. The cation distribution in crystal structure is important for various properties of materials as magnetic, catalytic etc.

The effect of synthesis temperature on ferrite formation and catalytic properties in reaction of methanol decomposition has been studied for  $\text{ZnFe}_2\text{O}_4$  composition [14]. It has been established that the crystallite size increases from 6 nm to 46 nm with

increasing of synthesis temperature from 300 °C to 700 °C. The catalytic activity of nanocrystalline  $\text{Cu}_{1-x}\text{Zn}_x\text{Fe}_2\text{O}_4$  synthesized at low temperature has been studied in [15]. It has been established that the mixed ferrite materials exhibit high catalytic activity in methanol decomposition and the catalytic behaviour of ferrites strongly depends on the phase transformations that occur by the influence of the reaction medium.

The aim of present work is to prepare well crystallized  $\text{Cu}_{1-x}\text{Zn}_x\text{Fe}_2\text{O}_4$  ferrites with different composition and to test their catalytic behaviour in methanol decomposition to CO and hydrogen. The influence of cation distribution in ferrites on the phase transformations under the reductive reaction medium and the relation with their catalytic properties was in the focus of the study.

### EXPERIMENTAL

Ferrite samples with compositions  $\text{Cu}_{1-x}\text{Zn}_x\text{Fe}_2\text{O}_4$  ( $x = 0.2, 0.5, 0.8$  or  $1.0$ ) were prepared by co precipitation method. The solution of  $\text{Cu}(\text{NO}_3)_2 \cdot 3\text{H}_2\text{O}$ ,  $\text{Zn}(\text{NO}_3)_2 \cdot 6\text{H}_2\text{O}$  and  $\text{Fe}(\text{NO}_3)_3 \cdot 9\text{H}_2\text{O}$  was precipitated with drop wise addition of 1 M  $\text{Na}_2\text{CO}_3$  up to  $\text{pH} = 9$  and continuous stirring. The obtained precipitate was washed with distilled water, dried at room temperature and treated at 973 K for 4 hours.

The powder XRD patterns were recorded using a TUR M62 diffractometer with Co K $\alpha$  radiation. The average crystallite size (D), the degree of microstrain and the lattice parameters were determined

\* To whom all correspondence should be sent:  
E-mail: nikivelinov@ic.bas.bg

by using the PowderCell-2.4 software [16]. The Transmission Mössbauer spectra (TMS) were obtained with a Wissel (Wissenschaftliche Elektronik GmbH, Germany) electromechanical spectrometer working in a constant acceleration mode. A  $^{57}\text{Co}/\text{Rh}$  source and a  $\alpha\text{-Fe}$  standard were used. The parameters of hyperfine interaction such as isomer shift (IS), quadrupole splitting (QS), effective internal magnetic field ( $H_{\text{eff}}$ ), line widths (FWHM), and relative weight (G) of the partial components in the spectra were determined using the Confit2000 software [17]. Methanol decomposition was carried out in a flow reactor at methanol partial pressure of 1.57 kPa and argon as a carrier gas (50 ml/min). The catalysts (0.055 g of catalyst) were tested under temperature-programmed regime within the range of 350–770 K and heating rate of 1 K/min. On-line gas chromatographic analyses were performed on a PLOT Q column using flame ionization and thermo-conductivity detectors.

## RESULTS AND DISCUSSION

The XRD data for the obtained  $\text{Cu}_{1-x}\text{Zn}_x\text{Fe}_2\text{O}_4$  ferrites (Fig. 1) revealed formation of well crystallized structure of cubic spinel phase at temperature used. A secondary phase identified as hematite was observed in the samples with high Cu content. The average crystallites size (D), degree of microstrain ( $\epsilon$ ) and lattice parameters determined from XRD patterns are presented in Table 1. The calculated crystalline size is in the range from 43 nm to 60 nm. The lattice parameters decrease from 8.43 to 8.39 Å when  $x$  in  $\text{Cu}_{1-x}\text{Zn}_x\text{Fe}_2\text{O}_4$  ferrites decreases from 1 to 0.2.

Mössbauer spectra of synthesized samples are presented in Fig. 2. The spectrum of pure  $\text{ZnFe}_2\text{O}_4$  exhibits of doublet corresponding to paramagnetic behaviour of zinc ferrite where all amount of  $\text{Fe}^{3+}$  ions are located in [B]-site of unit cell, while  $\text{Zn}^{2+}$  ions strongly prefer (A)-site position, determining

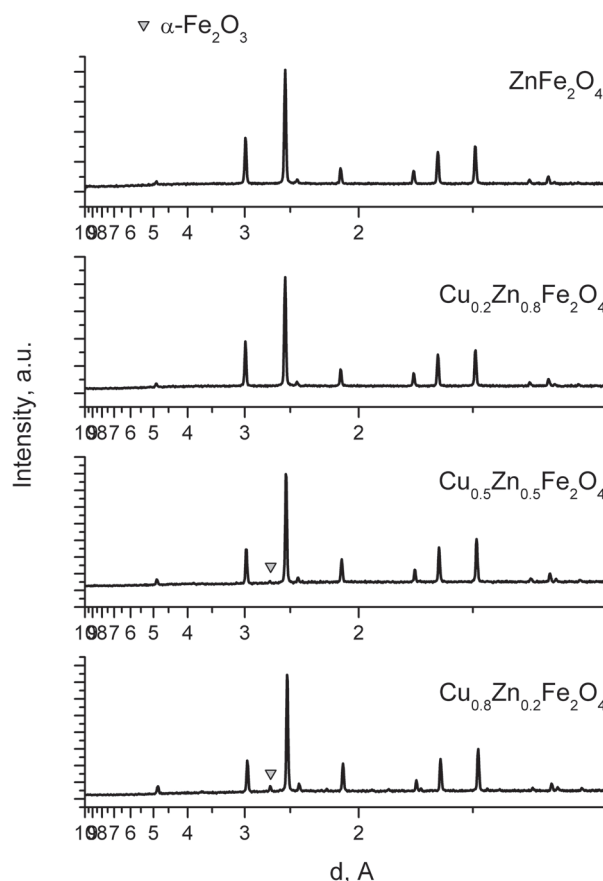


Fig. 1. X-ray diffraction patterns of synthesized samples

zinc ferrite as a normal spinel. The Mössbauer parameters show no significant difference of magnetic structure when  $x=0.8$  and existence of paramagnetic phase was also observed. Mössbauer spectra exhibit sextet magnetic components with copper content increase in samples  $\text{Cu}_{0.5}\text{Zn}_{0.5}\text{Fe}_2\text{O}_4$  and  $\text{Cu}_{0.8}\text{Zn}_{0.2}\text{Fe}_2\text{O}_4$ . In this case acceptable fitting of the experimental data could be obtained when the [B]-

Table 1. Average crystallite size (D), degree of microstrain ( $\epsilon$ ) and lattice parameters (a, c) determined from experimental XRD profiles

Sample	Phase	D, nm	$\epsilon \cdot 10^3$ , a.u	a, c, Å	%
$\text{ZnFe}_2\text{O}_4$	Fd3m(227) – cubic	45.84	1.187	8,43	100
$\text{Cu}_{0.2}\text{Zn}_{0.8}\text{Fe}_2\text{O}_4$	Fd3m(227) – cubic	59.82	1.684	8.42	100
$\text{Cu}_{0.5}\text{Zn}_{0.5}\text{Fe}_2\text{O}_4$	Fd3m(227) – cubic	42.80	0.352	8.41	98.6
	$\text{Fe}_2\text{O}_3$			a=5.04, c=13.77	1.4
$\text{Cu}_{0.8}\text{Zn}_{0.2}\text{Fe}_2\text{O}_4$	Fd3m(227) – cubic	45.24	0.997	8.39	91.3
	$\text{Fe}_2\text{O}_3$			a=5.03, c=13.77	8.7

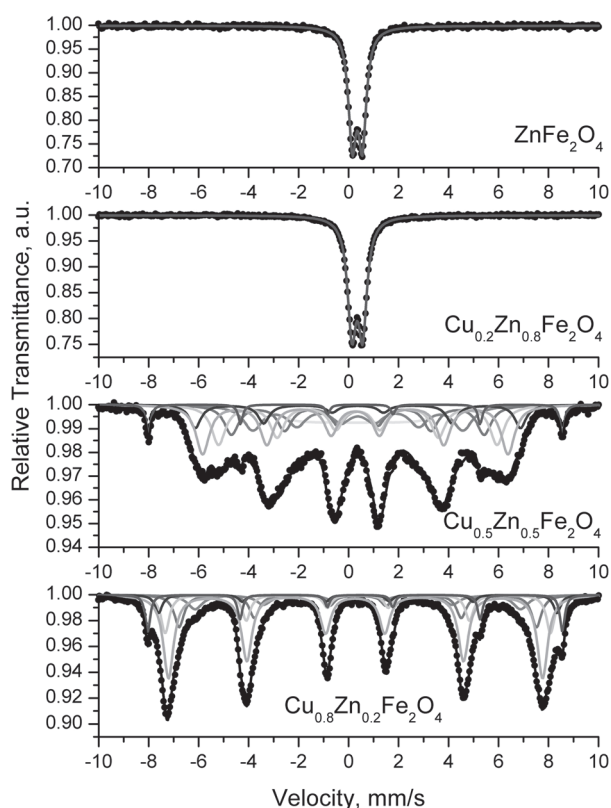


Fig. 2. Mössbauer spectra of synthesized samples

site pattern is assumed as superposition of more than one sextet. The binomial formula is used to calculate a probability  $P(n, x)$  of an octahedral site having  $n$  nearest-neighbor zinc atoms in order to define the

number of sextet components that have to use in the fitting model, as it has been used in [18]. Mössbauer spectra of one sextet referred to tetrahedral coordination of  $\text{Fe}^{3+}$  ions (A)-site and five sextets for  $x=0.5$  and four sextet for  $x=0.2$  with parameters of  $\text{Fe}^{3+}$  ions in octahedral position. The existence of number of sextet components with different hyperfine field can be explain with random occupancy of tetrahedral positions by  $\text{Fe}^{3+}$  and diamagnetic  $\text{Zn}^{2+}$  ions, results in existence of different (A)-site nearest neighbors of [B]-site  $\text{Fe}^{3+}$  i.e. 6Fe, 5Fe and 1Zn, 4Fe and 2Zn and etc. (A)-site neighbors (corresponding sextet components are shown in Table 2, as B0, B1, B2 and etc., followed by calculated probability in parenthesis). Additional sextet with parameters typical for hematite was determined in Cu- rich samples, as its relative weight is 4% and 8% for  $x=0.5$  for  $x=0.2$  samples respectively.

Temperature dependencies of methanol conversion and CO selectivity for various ferrite materials are presented in Fig. 3. The main registered by-products during the decomposition are  $\text{CO}_2$  (up to 20–30%) and  $\text{CH}_4$  (up to 2–10%). Note that the catalytic activity of the samples is in complex relation with their initial composition. The replacement of Zn with small amount of Cu leads to a decrease in the catalytic activity as compared to pure  $\text{ZnFe}_2\text{O}_4$ . However, the conversion curve of the sample with the highest copper content,  $\text{Cu}_{0.8}\text{Zn}_{0.2}\text{Fe}_2\text{O}_4$ , is shifted to 80–100 K lower temperature, indicating much higher catalytic activity. Mössbauer study of the samples after the catalytic test was carried out. For all materials significant phase transformations under the reaction medium are established. Formation

Table 2. Parameters of Mössbauer spectra of the investigated samples

Sample	Components	IS mm/s	QS mm/s	$H_{\text{eff}}$ , T	FWHM mm/s	G,%
$\text{ZnFe}_2\text{O}_4$	Db	0.35	0.40	–	0.38	100
$\text{Cu}_{0.2}\text{Zn}_{0.8}\text{Fe}_2\text{O}_4$	Db	0.35	0.43	–	0.42	100
$\text{Cu}_{0.5}\text{Zn}_{0.5}\text{Fe}_2\text{O}_4$	Sx1- $\text{Fe}_2\text{O}_3$	0.37	-0.20	51.4	0.22	4
	Sx2-tetra, A	0.27	0.00	37.0	0.65	23
	Sx3-octa, B1(0.09)	0.37	0.00	40.4	0.55	8
	Sx4-octa, B2(0.23)	0.37	0.00	34.6	0.68	19
	Sx5-octa, B3(0.31)	0.37	0.00	31.4	0.70	15
	Sx6-octa, B4(0.23)	0.37	0.00	26.1	0.93	16
	Sx7-octa, B5(0.09)	0.37	0.00	15.4	0.02	14
$\text{Cu}_{0.8}\text{Zn}_{0.2}\text{Fe}_2\text{O}_4$	Sx1- $\text{Fe}_2\text{O}_3$	0.36	-0.20	51.5	0.24	8
	Sx2-tetra, A	0.272	0.02	46.5	0.50	46
	Sx3-octa, B0(0.26)	0.37	0.00	49.5	0.36	6
	Sx4-octa, B1(0.39)	0.37	0.00	47.9	0.40	15
	Sx5-octa, B2(0.25)	0.37	0.00	44.4	0.47	15
	Sx6-octa, B3(0.08)	0.37	0.00	40.5	0.71	10

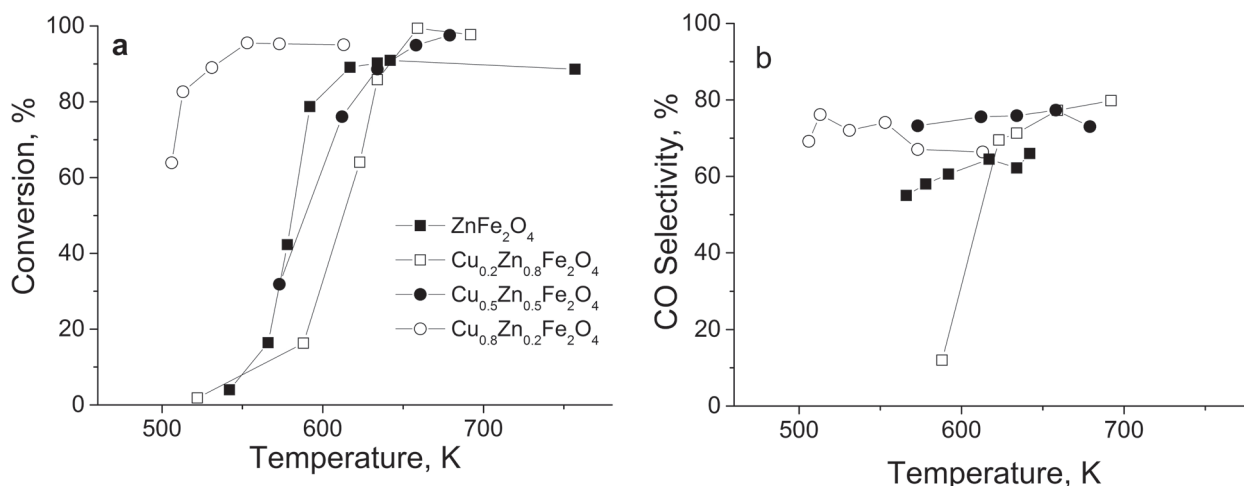


**Fig. 3.** Methanol conversion (a) and CO selectivity (b) vs. temperature of investigated ferrite materials

of metallic Fe and FeO is typical for pure  $\text{ZnFe}_2\text{O}_4$ , while metal-substituted magnetite ( $\text{Me}_x\text{Fe}_{3-x}\text{O}_4$ ,  $\text{Me} = \text{Cu}, \text{Zn}$ ) and  $\chi\text{-Fe}_5\text{C}_2$  and  $\theta\text{-Fe}_3\text{C}$  carbides in different ratio are observed for all bi-component ferrites (Fig. 4, Table 3). The relative part of  $\theta\text{-Fe}_3\text{C}$  is the highest for the sample with minimum copper content,  $\text{Cu}_{0.2}\text{Zn}_{0.8}\text{Fe}_2\text{O}_4$ . Formation of  $\chi\text{-Fe}_5\text{C}_2$  and

$\text{Me}_x\text{Fe}_{3-x}\text{O}_4$ , with the increase of the relative part of the latter is observed with copper content increase in ferrites. We assume that the highest catalytic activity of  $\text{Cu}_{0.8}\text{Zn}_{0.2}\text{Fe}_2\text{O}_4$  could be related to the formation of metal-substituted magnetite. A synergistic activity of this magnetite and finely dispersed copper particles is not excluded as well.

**Table 3.** Parameters of Mössbauer spectra of the investigated samples after catalytic test

Sample	Components	IS, mm/s	QS, mm/s	Heff, T	FWHM, mm/s	G, %
$\text{ZnFe}_2\text{O}_4\text{-MD}$	Sx1 – $\text{Me}_x\text{Fe}_{3-x}\text{O}_4$	0.28	-0.02	48.2	0.26	11
	Sx2 – $\text{Me}_x\text{Fe}_{3-x}\text{O}_4$	0.63	0.00	44.6	0.63	28
	Sx3 – $\alpha\text{-Fe}$	0.00	0.01	32.7	0.27	23
	Sx4 – $\theta\text{-Fe}_3\text{C}$	0.17	0.07	20.4	0.36	8
	Db – FeO	0.88	0.73	–	0.60	30
$\text{Cu}_{0.2}\text{Zn}_{0.8}\text{Fe}_2\text{O}_4\text{-MD}$	Sx1 – $\text{Me}_x\text{Fe}_{3-x}\text{O}_4$	0.26	-0.01	47.8	0.34	7
	Sx2 – $\text{Me}_x\text{Fe}_{3-x}\text{O}_4$	0.57	0.00	42.8	1.13	20
	Sx3 – $\theta\text{-Fe}_3\text{C}$	0.19	0.03	20.8	0.45	60
	Db – $\text{ZnFe}_2\text{O}_4$	0.36	0.36	–	0.39	13
$\text{Cu}_{0.5}\text{Zn}_{0.5}\text{Fe}_2\text{O}_4\text{-MD}$	Sx1 – $\text{Me}_x\text{Fe}_{3-x}\text{O}_4$	0.30	0.07	46.9	0.56	8
	Sx2 – $\text{Me}_x\text{Fe}_{3-x}\text{O}_4$	0.62	0.00	42.5	0.85	12
	Sx3 – $\chi\text{-Fe}_5\text{C}_2$	0.21	0.05	21.0	0.50	44
	Sx4 – $\chi\text{-Fe}_5\text{C}_2$	0.18	-0.00	18.8	0.49	15
	Sx5 – $\chi\text{-Fe}_5\text{C}_2$	0.17	0.01	11.5	0.36	7
	Sx6 – $\text{Cu}_{0.5}\text{Zn}_{0.5}\text{Fe}_2$	0.38	0.00	37.9	0.59	6
	Sx7 – $\text{Cu}_{0.5}\text{Zn}_{0.5}\text{Fe}_2$	0.28	0.00	32.2	1.06	8
$\text{Cu}_{0.8}\text{Zn}_{0.2}\text{Fe}_2\text{O}_4\text{-MD}$	Sx1 – $\text{Me}_x\text{Fe}_{3-x}\text{O}_4$	0.28	-0.01	48.0	0.32	15
	Sx2 – $\text{Me}_x\text{Fe}_{3-x}\text{O}_4$	0.60	-0.01	43.8	0.94	44
	Sx3 – $\chi\text{-Fe}_5\text{C}_2$	0.23	0.09	21.4	0.50	23
	Sx4 – $\chi\text{-Fe}_5\text{C}_2$	0.17	0.03	18.8	0.44	15
	Sx5 – $\chi\text{-Fe}_5\text{C}_2$	0.16	0.01	10.8	0.32	3

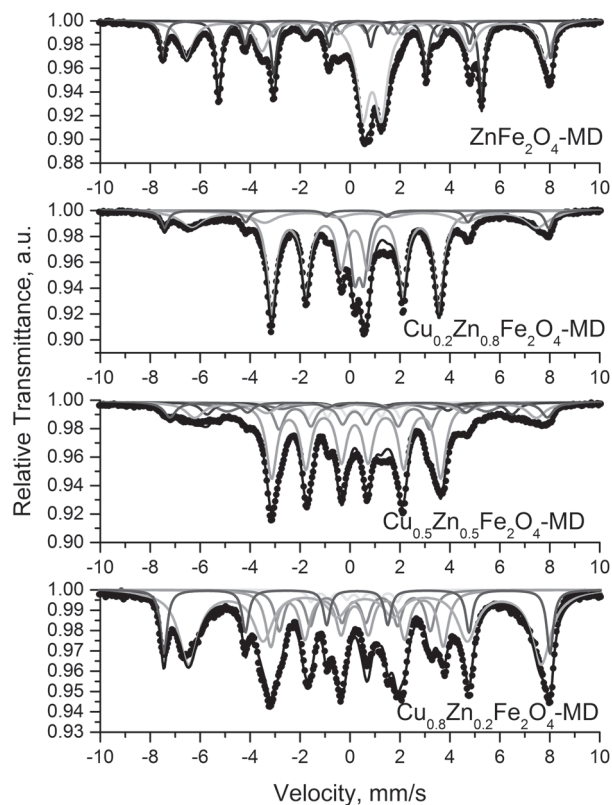


Fig. 4. Mössbauer spectra of samples after catalytic test

## CONCLUSIONS

Well crystallized  $\text{Cu}_{1-x}\text{Zn}_x\text{Fe}_2\text{O}_4$  ferrites with different composition were synthesized using co-precipitation method. The ferrite samples with higher Cu content exhibit better catalytic activity in methanol decomposition. Mössbauer study of the samples after the catalytic test reveals significant changes in the initial ferrite phase with the formation of metal-substituted magnetite, iron carbide, wuestite and  $\alpha\text{-Fe}$  in different ratio. The catalytic activity of ferrites correlates with their phase transformations by the influence of the reaction medium and facilitated effect of the formation of metal-substituted magnetite is established.

**Acknowledgements:** *The present work is financially supported by the Bulgarian National Science Fund under Projects DFNI-E01/7/2012 and FNI-E02/17/2014.*

## REFERENCES

1. K. E. Scarberry, E. B. Dickerson, Z. J. Zhang, B. B. Benigno, J. F. McDonald, *Nanomedicine: Nanotechnology, Biology, and Medicine*, **6**, 399 (2010).
2. M. N. Ashiq, F. Naz, M. A. Malana, R. S. Gohar, Z. Ahmad, *Mater. Res. Bull.*, **47**, 683 (2012).
3. K. Mukherjee, S. B. Majumder, *Sensor Actuator B-Chem*, **162**, 229 (2012).
4. A. Goldman, *Electronic Ceramics*, L. Levenson (ed.), Marcel Dekker, New York, 1988, p. 170.
5. C. Fauteux-Lefebvre, N. Abatzoglou, J. Blanchard, F. Gitzhofer, *J. Power Sources*, **195**, 3275 (2010).
6. R. Benrabaa, H. Boukhlof, S. Barama, E. Bordes-Richard, R. N. Vannier, A. Barama, *Catal. Lett.*, **142**, 42, (2012).
7. A. S. Albuquerque, M. V.C. Tolentino, J. D. Ardisson, F. C. C. Moura, R. de Mendonc, W. A. A. Macedo, *Ceram. Int.*, **38**, 2225 (2012).
8. X. Tana, G. Li, Y. Zhao, C. Hu, *J. Alloy. Compd.*, **493**, 55 (2010).
9. M. Mokhtar, S. N. Basahel, Y. O. Al-Angary, *J. Alloy. Compd.*, **493**, 376 (2010).
10. N. van Vegten, T. Baidya, F. Krumeich, W. Kleist, A. Baiker, *Appl. Catal. B- Environ.*, **97**, 398 (2010).
11. J. Chen, W. Shi, J. Li, *Catal. Today*, **175**, 216 (2011).
12. M. Massa, R. Häggblad, A. Andersson, *Top. Catal.*, **54**, 685 (2011).
13. B. Jäger, A. Stolle, P. Scholz, M. Müller, B. Ondruschka, *Appl. Catal. A-Gen.*, **403**, 152 (2011).
14. K. Koleva, N. Velinov, T. Tsoncheva, I. Mitov, B. Kunev, *Bulg. Chem. Commun.*, **45**, 434 (2013).
15. K. Koleva, N. Velinov, T. Tsoncheva, I. Mitov, Mössbauer study of  $\text{Cu}_{1-x}\text{Zn}_x\text{Fe}_2\text{O}_4$  catalytic materials, *Hyperfine Interact.*, **226**, 89 (2014).
16. W. Kraus, G. Nolze, *PowderCell for Windows*, Federal Institute for Materials Research and Testing, Berlin, 2000.
17. T. Žák, Y. Jirásková, CONFIT: Mössbauer spectra fitting program, *Surf. and Interface Anal.*, **38**, 710 (2006).
18. N. Velinov, E. Manova, T. Tsoncheva, Cl. Estournès, D. Paneva, K. Tenchev, V. Petkova, K. Koleva, B. Kunev, I. Mitov, *Solid State Sci.*, **14**, 1092 (2012).

## ПОЛУЧАВАНЕ, СТРУКТУРА И КАТАЛИТИЧНИ СВОЙСТВА НА МЕД-ЦИНКОВИ ФЕРИТИ

К. В. Колева<sup>1</sup>, Н. И. Велинов<sup>1\*</sup>, Т. С. Цончева<sup>2</sup>, И. Г. Митов<sup>1</sup>

<sup>1</sup> *Институт по катализ, Българска академия на науките, ул. Акад. Г. Бончев, бл. 11, 1113 София, България*

<sup>2</sup> *Институт по органична химия с център по фитохимия, Българска академия на науките, ул. Акад. Г. Бончев, бл. 9, 1113 София, България*

Постъпила декември, 2014 г.; приета януари, 2015 г.

(Резюме)

Добре кристализирани ферити със състав  $\text{Cu}_{1-x}\text{Zn}_x\text{Fe}_2\text{O}_4$  са получени и тествани като катализатори в реакцията на разлагане на метанол до СО и водород. Във фокуса на изследването са изучаването на влиянието на катионното разпределение във феритите върху каталитичното поведение и фазовите превръщания под влияние на реакционната среда. Установено беше, че феритът със състав  $\text{Cu}_{0.8}\text{Zn}_{0.2}\text{Fe}_2\text{O}_4$  проявява най-висока каталитична активност и добра селективност при разлагане на метанол до  $\text{H}_2$  и СО. Мьосбауеровият анализ на образците след каталитичен тест показва превръщане на първоначалната феритна фаза в следните фази: Zn-заместен магнетит, железен карбид, вюстит и  $\alpha$ -Fe.